

Precision Spectral Sculpting of Broadband FM Pulses Amplified in a Narrowband Medium

Solid-state laser systems envisioned for inertial fusion energy (IFE) applications will require both high efficiency and high single-beam, on-target uniformity. High efficiency is achieved by diode pumping, and on-target uniformity is achieved by beam-smoothing techniques. One of the most-promising gain media for these high-efficiency lasers is ytterbium-doped strontium fluorapatite ($\text{Yb}^{+3}:\text{SFAP}$).¹ While this material is ideal for efficient diode pumping, its gain bandwidth is relatively narrow. This has implications for the amount of on-target beam smoothing that can be achieved with techniques such as smoothing by spectral dispersion (SSD),² which requires bandwidths of the order of 1 THz in the ultraviolet³ or roughly 0.333 THz (330 GHz) in the infrared part of the system.⁴ Since this bandwidth is comparable to the gain bandwidth of $\text{Yb}^{+3}:\text{SFAP}$, significant gain narrowing can be expected in the laser system.

Gain narrowing in this case does more than limit the amount of on-target bandwidth available for beam smoothing. The technique of SSD impresses frequency-modulated (FM) bandwidth on the laser and disperses it with gratings in order to smooth speckle on target. Gain narrowing modifies this FM spectrum, leading to amplitude modulation (AM) or FM-to-AM conversion in the temporal profile of the pulse. The AM occurs primarily at the high-peak-power output of the laser system, significantly increasing the risk of laser damage.

In this article, the application of spectral sculpting to FM pulses is presented. Specifically, spectral sculpting is used to precompensate the effects of gain narrowing in narrowband solid-state amplifiers. The technique of spectral sculpting has previously been used to compensate the effects of gain narrowing in ultrafast amplifiers by spectrally shaping the input pulse prior to amplification⁵ or by the use of an intra-amplifier spectral filter.⁶ In these examples, the primary goal was to increase the width of the amplified output spectrum. For FM pulses, however, any modification to the original spectrum leads to AM; thus the effects of gain narrowing must be *precisely* compensated to ensure that the amplified output spectrum matches exactly the original, unamplified FM spec-

trum. We experimentally demonstrate complete gain-narrowing compensation for small-signal, center-line gains of the order of 10^4 and FM bandwidths that are comparable to the linewidth of the amplifying medium.

The concept of spectral sculpting is illustrated in Fig. 90.28. The spectrum of an FM pulse and its corresponding smooth temporal profile are shown in Fig. 90.28(a). As illustrated in Fig. 90.28(b), a spectral mask that attenuates the line-center sidebands, which experience high gain, and wholly transmits the distant low-gain sidebands is applied to the pulse at the input to the laser system. After spectral sculpting, this low-energy input pulse no longer has a purely FM spectrum and is thus heavily amplitude modulated [Fig. 90.28(b)]. As the pulse is amplified through the system, the sculpted spectrum evolves toward a purely FM spectrum. At the output of the

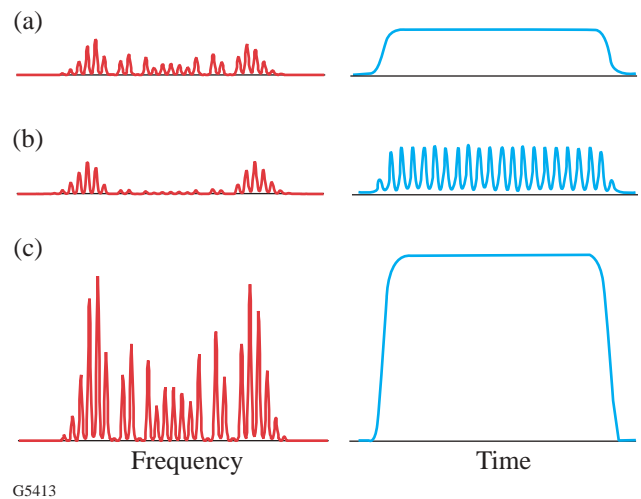
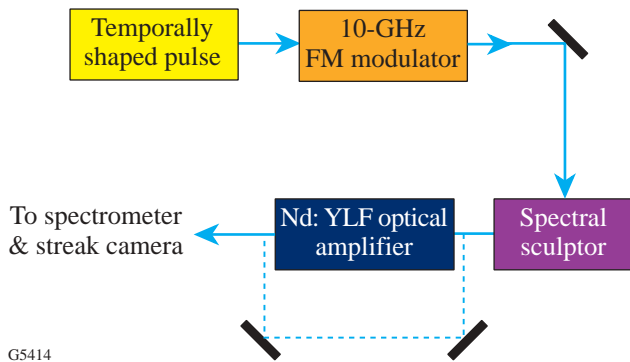


Figure 90.28
(a) Unamplified FM spectrum and associated smooth temporal profile. (b) Sculpted, unamplified FM spectrum. The associated temporal profile shows significant AM. (c) Sculpted, amplified FM spectrum. The amplified output has the original FM spectrum and a smooth temporal profile.

system, precisely where the energy, fluence, and concomitant damage risk are highest, the purely FM spectrum is recovered, with no AM [shown in Fig. 90.28(c)].

A schematic of the experimental setup is shown in Fig. 90.29. The FM bandwidth was generated by double passing a monochromatic, temporally shaped pulse through a LiNbO₃ phase modulator.⁷ This pulse then entered the spectral sculptor. After sculpting, the pulse was injected into a narrowband, cavity-dumped, multipass Nd:YLF amplifier. Nd:YLF's narrower gain transition serves as a surrogate for the Yb³⁺:SFAP with a proportional reduction in input bandwidth. The total number of round-trips through the cavity, and thus the overall gain experienced by the pulse, was adjustable. After amplification, the spectral profile of the sculpted, amplified pulse was measured with a custom-built spectrometer with a resolution of ~0.1 Å. To assess the magnitude of post-amplification AM, the temporal profile of these pulses was characterized with an LLE-built streak camera with a 15- to 20-ps temporal resolution.

The design of the spectral sculptor is based on a configuration known as a *zero-dispersion pulse compressor with a pulse-shaping mask*.⁸ In this configuration, the sidebands of the FM-modulated incident pulse are first angularly dispersed by a gold-coated diffraction grating. A lens then transforms the angular dispersion of the sidebands into a spatially separated array of individual sidebands located at the back focal (Fourier) plane of the lens. A mask, placed in this plane, performs the actual sculpting. The second half of the sculptor is a mirror image of the first part, producing a spectrally sculpted pulse whose individual FM sidebands are overlapped in space.



G5414

Figure 90.29
Schematic of the spectral sculpting setup.

The specific layout of a particular Fourier-plane mask dictates the optical design of the sculptor. Many types of both fixed and programmable masks might be used to shape the spectrum of a pulse.⁹ The programmable mask used here (from Cambridge Research Inc.) is based on the liquid-crystal-modulator (LCM) light valve developed by Wefers and Nelson.¹⁰ The discrete nature of the FM spectrum is ideally suited to this pixelated light valve, and thus our sculptor was designed so that the spatial separation between each sideband in the Fourier plane matched exactly the LCM pixel separation. For a grating groove density of 1740 grooves/mm, a center wavelength of 1.053 mm, an FM sideband spectral separation of 10.384 GHz, and a LCM pixel separation of 100 mm, the required focal length of the lenses was 775 mm. Since the required focal length was so long, each lens in the sculptor was replaced with a three-lens, telephoto system (designed by D. Weiner), resulting in a 60% reduction in the overall length of the sculptor.

The LCM light valve provides control of both the transmission and relative optical phase of each FM sideband. This is done by applying a computer-controlled voltage to each of two liquid crystal layers in each LCM pixel. The sculpting mask can thus be tailored to compensate a variety of conditions in the amplifier. An algorithm was developed that adjusts the transmission of each LCM pixel until the power spectrum of the amplified, sculpted pulse matches a given, desired reference spectrum.

The reference spectrum, which is the original pure FM spectrum generated by the phase modulator, was measured by sending the output of the sculptor, with the transmission of each LCM pixel set to 100%, directly to the spectrometer (see the dashed line in Fig. 90.29). Once the reference spectrum was taken, the unsculpted pulse was then amplified in the Nd:YLF amplifier and sent into the spectrometer. The power spectrum of the amplified pulse is given by

$$|E_{\text{amp}}(t)|^2 = |E_{\text{in}}(t)g(t)|^2, \quad (1)$$

where $|E_{\text{in}}(t)|^2$ is the spectrum of the unamplified, unsculpted pulse (the reference spectrum) and $|g(t)|^2$ is the gain spectrum of the Nd:YLF amplifier. Given this measurement of the amplified power spectrum, a compensating mask function $M(t)$ was then calculated and sent to the LCM. When the LCM is used only as a transmission mask, this mask function can be expressed as

$$M(I) = \frac{|E_{in}(I)|^2}{|E_{amp}(I)|^2} = \frac{1}{|g(I)|^2}. \quad (2)$$

The now-sculpted pulse was amplified, and the resulting spectrum was again measured and compared to the reference spectrum. This procedure was repeated until the amplified, sculpted spectrum matched the original reference spectrum $|E_{in}(I)|^2$. This comparison of spectra was accomplished by calculating the relative difference in energy between corresponding sidebands in the reference and amplified spectra. When the rms average difference among all of the sidebands was less than 4%, the spectra were considered to be equivalent and the sculpting procedure ended.

Figure 90.30(a) shows the measured reference FM spectrum, containing ~29 sidebands with a bandwidth of ~220 GHz. Since the spectral width of the Nd:YLF gain curve is approximately two-thirds the width of that of Yb³⁺:SFAP, we used an FM bandwidth that was two-thirds of that required for a Yb³⁺:SFAP-based IFE laser system using SSD for beam smoothing. The pulse temporal profile corresponding to the reference spectrum in Fig. 90.30(a), as measured with the streak camera, is shown in Fig. 90.30(b). Without precompensation, as shown in Fig. 90.30(c), the amplified (gross small-signal, center-line gain ~9100) FM pulse spectrum is significantly narrowed. The temporal profile of this gain-narrowed, amplified FM pulse shows nearly 100% AM [Fig. 90.30(d)]. Due to the fact that gain narrowing leads to a symmetric distortion of the original FM spectrum, the predominant frequency of the AM is ~20 GHz, which is twice the phase-modulation frequency.

Beginning with the unsculpted, amplified spectrum in Fig. 90.30(c), the sculpting algorithm iterated, as described above, until the sculpted, amplified spectrum matched the reference spectrum. For gains of ~10⁴, four to five iterations were typically required. The resulting amplified and sculpted spectrum is shown in Fig. 90.30(e). This power spectrum shows that precompensating the effects of gain narrowing produces an amplified spectrum that matches the original unamplified FM power spectrum, thus providing the necessary bandwidth for on-target smoothing. As discussed above, the sculpting technique must also produce amplified pulses with a minimum amount of AM. As can be seen in Fig. 90.30(f), the applied spectral sculpting mask used to generate the spectrum

in Fig. 90.30(e) has significantly reduced the AM at the amplifier output; however, some residual 20-GHz AM remains.

To better understand the source of this residual AM, a model that uses the experimentally measured power spectra to calculate the expected temporal pulse profile was developed. These simulations showed that the relative amplitude errors in the sidebands (which were typically of the order of a few percent) were not sufficient to cause the observed residual AM. It was thus concluded that the sculpting algorithm successfully produced the correct amplified FM power spectrum, and that the residual AM was not caused by errors in the sculpted amplitudes of the individual amplified sidebands.

The simulations described above were then expanded to include the effects of errors in the phase relationship among the sidebands that comprise the amplified FM spectra. Two primary sources of phase error in the experiment were material

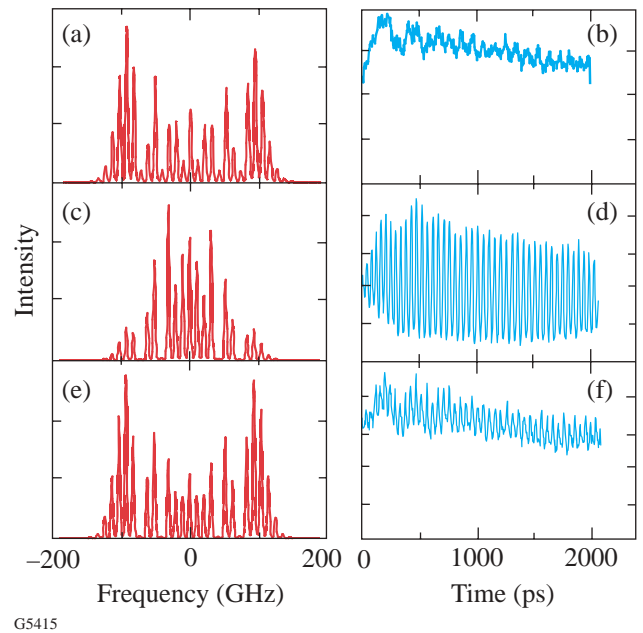


Figure 90.30 (a) Unamplified FM pulse spectrum (reference spectrum); (b) streak camera measurement of the temporal profile of the pulse whose spectrum is shown in (a); (c) gain-narrowed, amplified FM spectrum; (d) temporal profile corresponding to the gain-narrowed spectrum shown in (c); (e) amplified, sculpted FM spectrum; (f) temporal profile corresponding to the amplified, sculpted spectrum shown in (e).

dispersion and imaging errors in the sculptor. These sources primarily produce a spectral phase whose magnitude varies as the square of the frequency difference among the sidebands. Introducing this quadratic spectral phase dependence into our simulations produced FM pulses with amplitude modulation at the fundamental modulation frequency (i.e., 10 GHz). While a small amount of 10-GHz modulation can be observed in our data, the primary residual modulation frequency was 20 GHz.

Another source of spectral phase error in this setup is that associated with the narrowband Nd:YLF gain transition. Assuming that the gain profile of Nd:YLF is Lorentzian in shape, the spectral phase associated with this transition can be expressed as¹¹

$$f(\omega) = \frac{G_{dB}(\omega_c)}{8.68} \frac{2(\omega - \omega_c)/D\omega}{1 + [2(\omega - \omega_c)/D\omega]^2}, \quad (3)$$

where $G_{dB}(\omega_c)$ is the center-line gain in decibels, ω_c is the center frequency of the Nd:YLF transition, and $D\omega$ is its spectral FWHM. Simulations showed that the addition of a phase function of this form to an FM spectrum, using parameters that matched our experimental conditions, produced 20-GHz temporal modulation with an amplitude similar to that observed in the data.

Using our LCM sculptor, the amplitude mask used to produce the FM spectrum in Fig. 90.30(e) was combined with a phase mask whose functional form is the inverse of the function described by Eq. (3), with the overall gain, transition center frequency, and transition width being adjustable parameters. These parameters were iterated to minimize the amplitude modulation in the streak camera measurements. The resulting experimental temporal profile is shown in Fig. 90.31. Comparing this figure with Fig. 90.30(f), it is clear that by using phase compensation in addition to amplitude shaping, the residual AM in the amplified temporal pulse can be completely eliminated.

Conclusion

This article has presented what is believed to be the first demonstration of spectral sculpting applied to the amplification of broadband FM pulses in a narrowband gain medium. Because of FM-to-AM conversion, spectral sculpting for these pulses requires both precision amplitude and phase compensation of narrowband gain effects. Spectral sculpting for narrowband, center-line small-signal gains of 10^4 has been

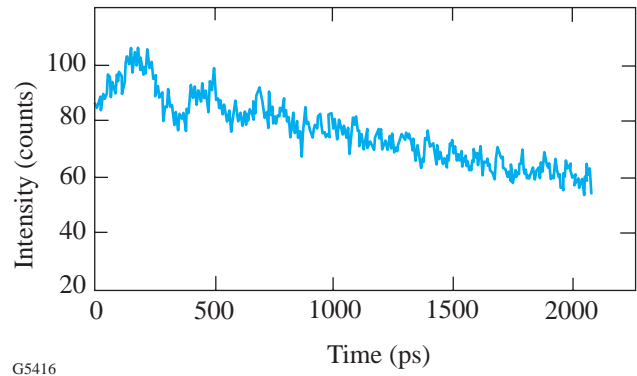


Figure 90.31

Temporal profile of an amplified FM pulse whose spectrum was both phase sculpted and amplitude sculpted.

demonstrated, producing amplified pulses that have both sufficient bandwidth for on-target beam smoothing and temporal profiles with no potentially damaging AM.

ACKNOWLEDGMENT

This work was supported by the U.S. Department of Energy Office of Inertial Confinement Fusion under Cooperative Agreement No. DE-FC03-92SF19460, the University of Rochester, and the New York State Energy Research and Development Authority. The support of DOE does not constitute an endorsement by DOE of the views expressed in this article.

REFERENCES

1. C. D. Marshall *et al.*, *IEEE J. Quantum Electron.* **32**, 650 (1996).
2. S. Skupsky, R. W. Short, T. Kessler, R. S. Craxton, S. Letzring, and J. M. Soures, *J. Appl. Phys.* **66**, 3456 (1989).
3. J. E. Rothenberg *et al.*, presented at the 1999 Fusion Summer Study Workshop, Snowmass, CO, 12–23 July 1999.
4. D. Eimerl *et al.*, *Opt. Lett.* **22**, 1208 (1997).
5. F. Verluise *et al.*, *Opt. Lett.* **25**, 575 (2000).
6. C. P. J. Barty *et al.*, *Opt. Lett.* **21**, 219 (1996).
7. Laboratory for Laser Energetics LLE Review **78**, 53, NTIS document No. DOE/SF/19460-295 (1999). Copies may be obtained from the National Technical Information Service, Springfield, VA 22161.
8. A. M. Weiner, J. P. Heritage, and E. M. Kirschner, *J. Opt. Soc. Am. B* **5**, 1563 (1988).
9. A. M. Weiner, *Rev. Sci. Instrum.* **71**, 1929 (2000).
10. M. M. Wefers and K. A. Nelson, *Opt. Lett.* **20**, 1047 (1995).
11. A. E. Siegman, *Lasers* (University Science Books, Mill Valley, CA, 1986), p. 283.